1 Inhibition of Streptococcus pneumoniae growth by

2 masarimycin.

- Brad A Haubrich^{a,d#}, Saman Nayyab^{a,e#}, Mika Gallati^a, Jazmeen Hernandez^a, Caroline Williams^a,
- 4 Andrew Whitmana, Tahl Zimmermanc, Qiong Lif, Yuxing Chenf, Cong-Zhao Zhouf, Amit Basubt,
- 5 Christopher W Reida*

```
6
               Center for Health and Behavioral Sciences
 7
                Dept. of Science and Technology
 8
               Bryant University
 9
               1150 Douglas Pike, Smithfield, RI 02917
10
                *Corresponding authors E-mail: <a href="mailto:creid@bryant.edu">creid@bryant.edu</a>, <a href="mailto:abasu@brown.edu">abasu@brown.edu</a>
11
               #both authors contributed equally to this work
12
13
        [b] Dept of Chemistry
14
               Brown University
15
               Providence, RI
16
        [c] Dept. of Family and Consumer Sciences
17
               North Carolina A&T State University
18
               Greensboro, NC
19
         [d] Touro University Nevada,
20
               College of Osteopathic Medicine, Dept of Basic Sciences
21
               Henderson, NV, 89014
22
         [e] University of Massachusetts Amherst
23
               Dept of Molecular and Cellular Biology
24
               230 Stockbridge Rd
25
               Amherst, MA
26
               School of Life Sciences
27
               University of Science and Technology of China
28
               Hefei, Anhui, 230027, P.R. China
```

Keywords: peptidoglycan, chemical biology, mode-of-action, meta-phenotype, cell wall

Abstract:

29

30 31

32

33

34 35

36

37

38

39

40

Despite renewed interest, development of chemical biology methods to study peptidoglycan metabolism has lagged in comparison to the glycobiology field in general. To address this, a panel of diamides were screened against the Gram-positive bacterium *Streptococcus pneumoniae* to identify inhibitors of bacterial growth. The screen identified the diamide masarimycin as a bacteriostatic inhibitor of *S. pneumoniae* growth with an MIC of 8 μM. The diamide inhibited detergent-induced autolysis in a concentration-dependent manner, indicating perturbation of peptidoglycan degradation as the mode-of-action. Cell based screening of masarimycin against a panel of autolysin mutants, identified a higher MIC against a Δ*lytB* strain

- lacking an endo-N-acetylglucosaminidase involved in cell division. Subsequent biochemical and
- 42 phenotypic analyses suggested that the higher MIC was due to an indirect interaction with LytB.
- 43 Further analysis of changes to the cell surface in masarimycin treated cells identified the
- overexpression of several moonlighting proteins, including elongation factor Tu which is
- implicated in regulating cell shape. Checkerboard assays using masarimycin in concert with
- 46 additional antibiotics identified an antagonistic relationship with the cell-wall targeting antibiotic
- fosfomycin, which further supports a cell-wall mode-of-action.

Introduction

- 49 Antibiotic resistance is a growing global threat. Drug-resistant *Streptococcus pneumoniae* alone
- is estimated to cause more than 2 million infections with an excess of 1.3 billion USD in medical
- costs per annum.[1, 2] In light of this, there is need for the development of new therapeutics.
- 52 Peptidoglycan (PG) is the primary structural heteropolymer conferring strength and cell shape
- 53 determination in both Gram-negative and Gram-positive organisms (Figure 1). The PG
- 54 polysaccharide backbone is composed of β-1,4-linked N-acetylmuramic acid (MurNAc) and N-
- 55 acetylglucosamine (GlcNAc). Attached to the C-3 lactyl moiety of MurNAc is a stem peptide
- that is involved in cross-linking the adjacent glycan strands to form the three-dimensional
- 57 structure of the cell wall. The incorporation of new material into the stress bearing layer of the
- 58 existing cell wall requires the delicate homeostasis of biosynthetic and degradative enzymes to
- 59 prevent lysis.[3, 4] Disruption of this interplay between degradative and biosynthetic enzymes
- 60 via chemical inhibition could provide unique insights into their biological role. The degradative
- 61 enzymes, collectively referred to as autolysins, are a broad class of enzymes that are
- 62 differentiated based on their bond selectivity. Deciphering physiological activity of autolysins
- has been a formidable task as functional redundancy complicates attribution of biological
- 64 activity.[5] Recent biophysical [4, 6] and computational studies [7] of bacterial autolysins have
- 65 begun to unravel their roles in the release of stress in the cell wall to allow for incorporation of
- 66 new material. A renaissance in PG metabolism research has started to provide new chemical
- 67 biology tools to study synthesis [8-11] and the role endopeptidases play in methicillin
- 68 resistance.[12] While the cell wall, and PG in particular, have provided a wealth of clinically
- 69 relevant antimicrobial targets [13], our understanding of the complex interplay between
- 70 degradative and synthetic steps is still developing.
- 71 Previously, we had screened a panel of 21 diamides for antibacterial activity against the Gram-
- 72 positive Bacillus subtilis.[14] This screen identified the diamide masarimycin (formerly fgkc)
- 73 (Figure 1 inset) as a bacteriostatic inhibitor of *B. subtilis* growth that targets the major active *N*-

acetylglucosaminidase (GlcNAcase) LytG (glycosyl hydrolase family 73 (GH73)) *in vitro*. Here we report on the screening of this panel of diamides against *S. pneumoniae*, identifying masarimycin as a bacteriostatic inhibitor of cell growth. Although an initial examination experiment implicates a related *S. pneumoniae* GlcNAcase (LytB, GH73) in masarimycin's activity, it is not the direct molecular target. A series of subsequent mode-of-action studies in *S. pneumoniae* highlights the challenges involved in target identification.

Materials and Methods

74

75

76

77 78

79

- Strains and compounds. Streptococcus pneumoniae 6305 and R6 were purchased from ATCC
- 82 (Mannassas, VA), and S. pneumoniae IU1945 (ΔlytB, ΔlytC, ΔdacA, ΔdacB, Δpmp23, Δpbp1a)
- 83 mutants were kindly provided by Dr. Malcolm E. Winkler at the University of Indiana.[15] S.
- pneumoniae TIGR4 and TIGR4 △lytB strains were previously reported.[16] S. pneumoniae
- strains were grown in Mueller Hinton (MH) broth (MilliporeSigma, St. Louis, MO) supplemented
- with 5 % (v/v) sheep blood (Lampire Biological, Pipersville PA) or MH agar plates containing 1.5
- 87 % (m/v) Bacto agar and 5 % (v/v) sheep blood at 37°C under anaerobic conditions.
- 88 Staphylococcus aureus was grown in MH broth or solid media, Clostridiodes difficile was grown
- in brain heart infusion (BHI) and *Escherichia coli* DH5α on Luria Bertani (LB) broth or solid
- 90 media. Diamide inhibitors were synthesized as described previously.[14] Other reagents, unless
- otherwise specified, were purchased from MilliporeSigma (St. Louis, MO).
- 92 MIC assays. MIC values were determined using the resazurin method.[17] Briefly, cells were
- 93 initially grown from the freezer on MH agar plates containing 5% defibrinated sheep blood. For
- all assays second passage cells of *S. pneumoniae* 6305, TIGR4, or R6 were used and grown
- overnight in MH broth, and standardized to an $OD_{600nm} = 0.4$. Inhibitors were analyzed *via* serial
- 96 dilution into PBS media in microtitre plates. For masarimycin, dilutions were initially made in
- 97 DMSO down to a concentration of 100 μM, further dilutions were then made into PBS. Plates
- 98 containing MH broth were inoculated with a 1/20 dilution of the OD_{600nm} = 0.4 cell culture with a
- 99 final concentration of 1 % DMSO. Cultures were grown statically under anaerobic conditions for
- 24 h at 37 °C, followed by addition of 30 μL of a 0.01% (m/v) solution of resazurin. The plates
- were incubated for 15 min to allow stabilization of color production. MICs were read directly off
- the plate; MICs were recorded as the lowest concentration that completely inhibited growth. MIC
- assays with *S. aureus* were performed in MH broth, *C. difficile* in BHI broth, while *E. coli* was
- performed in LB.

- 105 Morphological studies of S. pneumoniae. Cultures were prepared from second passage S. 106 pneumoniae 6305, R6 and △lytB [15] as previously described for MIC determination. Cells were washed in phosphate-buffered saline and chemically fixed in 20 mM HEPES pH 6.8 containing 107 1% formaldehyde. [18] Samples were fixed overnight at 4 °C to limit *de novo* cell wall 108 109 biosynthesis during fixation and stained with 0.1% (m/v) methylene blue (solution in 20% 110 ethanol). Samples were gently heated to 60 °C for 15-20 min to bring cells to a common focal plane. Slides were visualized using bright-field microscopy with a Zeiss Primo Star microscope 111 at 1000× magnification. Micrographs were acquired using an Axiocam ERc5s camera and Zen 112 lite software. 113
- Autolysis assays. Cellular autolysis assays were performed as previously described by Cornett and Shockman.[19] Briefly, *S. pneumoniae* 6305 were grown in MH broth containing 5% (v/v) defibrinated sheep blood under anaerobic conditions. Cells were harvested by centrifugation (8,000 rpm, 5 min) and washed with PBS. Cells were suspended in PBS and autolysis induced with the addition of Triton X-100 to a final concentration of 0.1% (v/v) and turbidity monitored at 600 nm over 60 min. Rates were calculated using the linear portion of the autolysis curves with the rate of autolysis in the absence of inhibitor set at 100%.
- Chain dispersing assay. Dispersion of the ΔlytB chain morphology with purified LytB was carried out as previously described using the TIGR4 and associated ΔlytB strains. [16] LytB was added to the cell suspension at a final concentration of 2 μM. The final concentration of masarimycin in the assays was 40 μM.
- DNA intercalation assays. To determine if masarimycin intercalates DNA, DNA mobility shift assays were performed as previously described using BamHI-linearized pUC18 plasmid.[20] The known DNA intercalator actinomycin D was used as a control.
- Dnase I assays. Degradation of the pUC18 plasmid DNA was assayed using 150 ng of linearized pUC18 plasmid as described by Huang et al.[21] Compound titrations in DMSO were added and reactions were initiated with 0.002 units of Dnase I. The reactions were incubated for 15 min at 37°C before being subjected to agarose gel electrophoresis. EDTA was used as a control for Dnase I inhibition.
- Lipotechoic acid detection by Western blot. Lipoteichoic acid profiles were analyzed as previously described.[22] Briefly, S. pneumoniae R6 cells were cultured overnight, harvested (3000 x g), resuspended in 6 M urea, and incubated at 37°C for 5 min to solubilize proteins.

 Samples were standardized by total protein content and separated by SDS-PAGE (16%) and

137 transferred to PVDF membrane. The membrane was incubated with a 1:5000 α-phosphocholine 138 monoclonal antibody (SSI Biotech, Santa Cruz, CA). Blots were analyzed by 139 chemiluminescence. Analysis of cell-wall associated proteins. Changes to cell wall protein profiles were analyzed as 140 previously described.[23] Briefly, second passage S. pneumoniae R6 were inoculated 1/100 into 141 MH broth and grown statically for 6 h anaerobically at 37°C. Masarimycin was added to a final 142 143 concentration of 0.75x MIC, the effect of solvent was controlled by the addition of DMSO to a 144 second flask and the cells grown overnight at 37°C anaerobically. Cells were harvested into PBS containing sucrose (20% w/v) and pelleted at 8,000 rpm for 10 min. The pellets were 145 146 washed with PBS containing 20% (w/v) sucrose and centrifuged again. The washed and 147 pelleted bacteria were resuspended in 2 mL of 50 mM glycine-NaOH (pH 12.0) containing 20% 148 (w/v) sucrose and incubated for 30 min at room temperature with gentle shaking. The suspension was centrifuged (10,000 rpm, 20 min). The supernatant was collected, and adjusted 149 150 to pH 7 with 1 M HCl, proteins precipitated with acetone and analyzed by 1D-SDS PAGE and silver staining. All lanes were standardized to total A_{280nm} loaded onto the gel. Bands were 151 152 excised from the gel and sent for identification by mass spectrometry at the National Resource 153 for Proteomics (University of Arkansas). 154 Proteomic analysis of SDS-PAGE gel bands. Each SDS-PAGE gel band was subjected to in-gel 155 trypsin digestion as follows. Gel segments were destained in 50% methanol, (Fisher), 50 mM ammonium bicarbonate, (Sigma-Aldrich), followed by reduction in 10 mM Tris[2-156 carboxyethyl]phosphine (Pierce) and alkylation in 50 mM iodoacetamide. (Sigma-Aldrich). Gel 157 slices were then dehydrated in acetonitrile, (Fisher), followed by addition of 100 ng porcine 158 sequencing grade modified trypsin (Promega) in 50 mM ammonium bicarbonate (Sigma-Aldrich) 159 160 and incubation at 37°C for 12-16 hours. Peptide products were then acidified in 0.1% formic acid. (Pierce). Tryptic peptides were separated by reverse phase Xselect CSH C18 2.5 um resin 161 (Waters) on an in-line 150 x 0.075 mm column using a nanoAcquity UPLC system (Waters). 162 Peptides were eluted using a 60 min gradient from 98:2 to 65:35 buffer A:B ratio. [Buffer A = 0.1%] 163 formic acid, 0.5% acetonitrile; buffer B = 0.1% formic acid, 99.9% acetonitrile.] Eluted peptides 164 165 were ionized by electrospray (2.4 kV) followed by MS/MS analysis using higher-energy collisional 166 dissociation (HCD) on an Orbitrap Fusion Tribrid mass spectrometer (Thermo) in top-speed data-167 dependent mode. MS data were acquired using the FTMS analyzer in profile mode at a resolution 168 of 240,000 over a range of 375 to 1500 m/z. Following HCD activation, MS/MS data were acquired

using the ion trap analyzer in centroid mode and normal mass range with precursor mass-

dependent normalized collision energy between 28.0 and 31.0. Proteins were identified by database search using Mascot (Matrix Science) with a parent ion tolerance of 3 ppm and a fragment ion tolerance of 0.5 Da. Scaffold (Proteome Software) was used to verify MS/MS based peptide and protein identifications. Peptide identifications were accepted if they could be established with less than 1.0% false discovery by the Scaffold Local FDR algorithm. Protein identifications were accepted if they could be established with less than 1.0% false discovery and contained at least 2 identified peptides. Protein probabilities were assigned by the Protein Prophet algorithm.[24]

177

170

171

172

173

174 175

- 178 Antagonism assay and fractional inhibitory concentration index (FIC_{Index}) determination.
- 179 Fractional inhibitory concentration index (FIC_{Index}) was conducted to determine the interaction
- 180 between masarimycin and a range of antibiotics with defined mode-of-action in a 96 well-plate
- 181 microdilution broth assay. A checkerboard assay was performed with each masarimycin pair as
- 182 previously described. [25] Plates were inoculated with 5 μL of a OD_{600nm} =0.2 culture of S.
- 183 pneumoniae R6 and growth monitored as previously described for the MIC assays. FICIndex was
- determined using the formulae: 184
- (Eq 1) $FIC = X/_{MICx}$, where X is the lowest inhibitory concentration of the drug in the 185
- presence of the co-drug, and MICx is the lowest inhibitory concentration of the drug in the 186
- 187 absence of the co-drug.
- 188 (Eq 2) FIC_{Index}= FIC_{masarimycin} + FIC_{antibiotic}
- 189 Drug interactions were rated as synergistic (FIC_{Index} \leq 0.5), additive (0.5 < FIC_{Index} \leq 1.0),
- indifferent (1.0 < FIC_{Index} ≤ 4.0), and antagonistic (FIC_{Index} > 4.0), based on published 190
- 191 standards.[26]
- NADP/NADP(H) ratio assays. Measurement of NADP/NADPH intracellular ratios was 192
- 193 determined via the Amplite colorimetric NADP/NADPH ratio assay kit (Kit #15274:, AAT
- Bioquest Inc, Sunnyvale CA) following manufacturer protocols. S. pneumoniae R6 second 194
- passage cells grown on MH with 5% defibrinated sheep blood under anaerobic conditions were 195
- used to inoculate 5 mL MH broth cultures ($OD_{600nm} = 0.5$) containing either masarimycin (1x, 3x 196
- 197 MIC) or vehicle control. Cultures were grown under anaerobic conditions for 1.5 h and
- centrifuged (8,000 rpm, 10 min). Cell pellets were resuspended in PBS and lysed via sonication. 198
- 199 Lysed cells were then used in assays following manufacturer's instructions. Samples were
- 200 analyzed in a 96 well plate format using a Molecular Devices SpectraMax190 with detection at
- 201 570 nm. Data was analyzed using GraphPad Prism.

Results and Discussion

202

203 We screened a previously reported [14] panel of 21 diamides against S. pneumoniae using the 204 resazurin microtiter assay (Figure S1).[17] Of the 21 compounds screened, masarimycin (formerly fgkc) was identified as a single digit micromolar bacteriostatic inhibitor (Figure S2) of 205 206 S. pneumoniae growth with an MIC of 8 µM against all three strains of S. pneumoniae that we tested - 6305, R6, and TIGR4 (Figure S3A). Three strains were chosen for screening to 207 208 account for the known genomic plasticity among S. pneumoniae isolates which can manifest as varying antibiotic sensitivity between strains. [27-29] TIGR4 was included as it is capable of 209 210 causing invasive disease.[30] These results for masarimycin are comparable to those obtained 211 against B. subtilis (MIC = 3.8 µM, bacteriostatic) [14] To further investigate masarimycin 212 spectrum, the compound was screened against the Gram-positive organisms Clostridiodes 213 difficile, Staphylococcus aureus and Gram-negative Escherichia coli which possess at least one GH73. In all cases, no antimicrobial activity was observed up to 150 µM (Figure S3B). 214 215 Extrapolating from the activity of masarimycin against *B. subtilis*, where it inhibits LytG, a GH73 enzyme, we hypothesized that the target of masarimycin in S. pneumoniae was also a GH73 216 family glycosidase. S. pneumoniae possesses one glycosidase classified as a member of the 217 218 GH73 family (www.cazy.org) – LytB, a cell division associated endo-β-GlcNAcase belonging to 219 cluster 4 of GH73.[16, 31-33] In contrast, B. subtilis LytG is an exo-acting GlcNAcase active in 220 vegetative growth and belongs to GH73 cluster 2.[34] 221 Given the potential connection to LytB and cell wall metabolism, we examined whether masarimycin inhibited autolytic activity in S. pneumoniae (Figure 2A). Exposure of S. 222 pneumoniae to low concentration of the non-ionic detergent (Triton X-100) induces 223 224 autolysis.[19] This autolytic activity was inhibited in a concentration-dependent manner by 225 masarimycin. The elevated concentration for near complete inhibition of autolysis in the whole 226 cell assay is likely due to the broad dysregulation of autolysins induced by Triton X-100. Given 227 the observed inhibition of autolytic activity, the MIC of masarimycin was determined for a series of S. pneumoniae mutant strains lacking the autolysins lytA, lytB, pmp23, dacA, or dacB, as well 228 229 as the bifunctional pbp1a. It has been demonstrated that deletion of any gene that affects PG 230 biosynthesis, stability, or regulation can make the bacterium more susceptible to compounds 231 that target the cell wall. [27] While none of the mutants were more sensitive to masarimycin, 232 higher MICs were observed with lytB (GH73 GlcNAcase), pmp23 (muramidase), and dacA 233 (pbp3, D,D-carboxypeptidase) mutants. This is counter to what was observed in a screen of 234 autolysin mutants in B. subtilis.[14] The near 4-fold decrease in sensitivity to masarimycin in the

236 to masarimycin. 237 To further explore these results, morphological changes induced by sub-MIC (0.7x) 238 concentrations of masarimycin, and antibiotics with known modes-of-action were investigated 239 (Figure S4). Treatment of S. pneumoniae with the cell wall-acting antibiotics bacitracin, 240 vancomycin, as well as the protein synthesis inhibitor kanamycin presented a phenotype of clumping cells. Sub-MIC treatment with masarimycin showed a change similar to these 241 antibiotics. The clumping phenotype observed with kanamycin has been associated with 242 243 antibiotics that target intracellular protein synthesis.[35] In light of this, the clumping phenotype 244 could not be directly attributed to a cell wall mode-of-action. Comparison of the masarimycininduced phenotype with the reported phenotypes of a ∆*lytB*[15], ∆*pmp*23[36], or ∆*dacA*[37] 245 mutants, for which higher MICs with masarimycin were observed, did not correlate, Additionally, 246 247 the masarimycin-induced phenotype did not correspond to phenotypes of other S. pneumoniae 248 autolysin mutants. [38-40] The masarimycin phenotype more closely resembles a morphology in 249 which the autolysin is still produced but is catalytically inactive, such as that reported for E61Q 250 and D68N mutants of pmp23. [36] 251 To further probe alterations to the cell wall suggested by the autolysis and genetic screen 252 assays, lipoteichoic acid (LTA) disruption was monitored by Western blot in the presence of 253 sub-MIC masarimycin. LTA has been shown to regulate autolysin activity in several species and 254 LytB possesses a choline binding domain, a component of S. pneumoniae LTA.[41-43] 255 Additionally, it has been suggested that LytB function is altered when cell wall choline content is 256 depleted.[44] Results indicated that changes to LTA and choline incorporation in the cell wall 257 was not a contributor to the observed masarimycin-induced autolysis, genetic screen, and morphology phenotypes (Figure S5A). 258 259 Next, changes to cell-wall-associated protein profiles were examined using high-pH extraction[23] of the S. pneumonia cell surface (Figure S5B). Upon treatment with 0.75x MIC 260 261 masarimycin the appearance of several overexpressed proteins was observed. Proteomic 262 analysis of SDS-PAGE gel bands identified several cell surface and moonlighting proteins that 263 are present only in the masarimycin treated sample (Table 1, Supplementary dataset 1). Of note 264 is the upregulation of elongation factor Tu, a known moonlighting protein that has been 265 implicated in regulating cell shape by modulating the formation of MreB filaments in B. subtilis 266 and E. coli.[45] The overexpression of proteins involved in complex carbohydrate catabolism 267 (BgaA, MalX) have been previously shown to be regulated by the two-component system

\(\Delta I vtB \) mutant suggests that changes to the cell wall imparted by the lack LytB reduces sensitivity

CiaR/H, which is also associated with sensing cell-wall stress in *S. pneumoniae*.[46] These changes to proteins on the cell surface suggest that masarimycin is interfering with cell wall remodeling.

Table 1. Overexpressed proteins observed in SDS-PAGE gel (Figure S5B) of *S. pneumoniae* R6 cell-surface protein extracts when exposed to 0.75x MIC masarimycin.

Gel	Protein ID	Biological Function	
Band			
1	1. BgaA β-galactosidase	Plays role in growth and adhesion[47]	
	2. Iga immunoglobin A1	2. Covalently linked to cell surface by sortase A.	
	protease	Involved in host immune evasion. [48]	
2	Spr0440, endo-β-GlcNAcase	Surface protein, role in commencement of	
		neuroinvasion[49]	
3	 Elongation factor Tu 	Moonlighting function in regulation of cell	
	2. PykF Pyruvate kinase	shape[50]	
		2. Moonlighting protein [51, 52]	
5	MalX maltooligosaccharide	Complex carbohydrate catabolism regulated by	
	transporter	CiaR/H system which is involved in sensing cell wall	
		stress.[46, 53]	
6	GapA glyceraldehyde 3-	Moonlighting protein[52]	
	phosphate dehydrogenase		

To further investigate the higher MIC observed with the $\Delta lytB$ mutant, inhibition of LytB activity was investigated in an established chain dispersing assay using the TIGR4 $\Delta lytB$ strain in the presence of exogenously added LytB.[16] When the $\Delta lytB$ mutant was treated with exogenous LytB, dispersion of the chains was observed (Figure 3). When a 5-fold MIC (40 μ M) concentration of masarimycin was added, LytB catalyzed chain dispersion was not inhibited. In vitro analysis with Remazol Brilliant Blue labeled PG [16, 54] and purified LytB confirmed these results. This lack of inhibition of the biochemical activity of purified LytB further suggests that the higher MIC of masarimycin observed for the $\Delta lytB$ mutant may be due to changes in cell wall structure, stability, or metabolism. These results further highlight the difficulty in target identification of small molecule inhibitors. The reduced MIC values observed in the genetic screen against the $\Delta lytB$ strain is is likely due to a more complex interplay between the deletion

of LytB and the actual target(s) of masarimycin. Consistent with this hypothesis, treatment of $\triangle lytB$ with 0.7x MIC masarimycin (Figure 4) resulted in the conversion of the $\triangle lytB$ chaining phenotype to the clumping phenotype observed in Figure S4. Co-administration of sub-MIC concentrations of cefoxitin, a DacA (PBP3) selective β-lactam, with masarimycin resulted in the reduction of the clumping phenotype in the *\(\Delta\) lytB* mutant but not wildtype cells. This further suggests that masarimycin's mode-of-action is impacted by alterations to the cell wall caused by either genetic deletion or chemical inhibition of autolysins. LytB is implicated in PG remodeling during cell division while DacA is associated with division rather than remodeling. [15] These observations suggest that masarimycin is influencing cell wall biosynthesis, turnover, stability, and/or regulation in these mutant backgrounds. Given their roles in cell wall remodeling during division (LytB) or directly involved in division or division complex (DacA, Pmp23) and the overexpression of elongation factor Tu suggests that masarimycin is either directly or indirectly impacting the cell wall during division. Taken collectively, the reduction in autolysis, phenotypic changes and overexpression of surface associated proteins observed with masarimycin, along with the reduced sensitivity against multiple mutant strains, suggest that these results could be the result of meta-phenotypes - a phenotype that results from the alteration of more than one pathway.[55] For instance, the clumping meta-phenotype observed in S. pneumoniae in the presence of masarimycin could be generated via a direct mechanism (e.g. inhibition of an enzyme associated with cell wall metabolism) or an indirect one (e.g. alterations in autolysin expression levels, changes in metabolic flux through cell wall associated pathways). To further interrogate the potential mode-of-action, masarimycin was screened in checkerboard

285

286

287288

289

290

291

292

293

294295

296297

298

299

300

301

302 303

304

305

306

307

308

309 310

311312

313

314

315

316317

To further interrogate the potential mode-of-action, masarimycin was screened in checkerboard assays with antibiotics with well-defined mechanisms (Table 2). Using pre-established guidelines [26] for interpreting FIC_{Index}, two antibiotics, levofloxacin (DNA gyrase) and fosfomycin (MurA, first committed step of PG biosynthesis) demonstrated mild antagonism (FIC_{Index} 4.5). Antagonistic relationships can be used to map genetic networks and reveal novel connections between pathways.[25] Antagonism with fosfomycin suggests a functional connection to the target of masarimycin. To further probe the antagonism with fosfomycin, we looked to see if masarimycin was indirectly impacting fosfomycin's target MurA. The subsequent step, catalyzed by MurB reduces the product of MurA, UDP-GlcNAc-enolpyruvate, to UDP-MurNAc utilizing NADPH. [56] Given the impact that changes to the cell wall have on masarimycin activity, we wondered if the observed antagonism with fosfomycin might be due to altered redox potential in the cell, a consequence of a destabilized cell envelope. This could

319 Alterations in redox potential and oxidative stress can negatively influence fosfomycin 320 sensitivity.[57] It has been previously demonstrated in S. aureus that alterations in metabolic flux of precursors and cofactors can contribute to fosfomycin resistance.[58] Changes in 321 322 NADP/NADPH levels were measured in a colorimetric assay in the presence/absence of 323 masarimycin. The ratio of NADP/NADPH did not change when up to 3x MIC masarimycin was 324 present (Figure S6) suggesting the fosfomycin antagonism is not due to an altered redox 325 potential impacting flux through MurB. Antagonism with levofloxacin provides a counterpoint to the fosfomycin results. Levofloxacin 326 327 introduces double-stranded DNA breaks upon inhibition of DNA gyrase, and induces the SOS 328 response system.[59] To further evaluate this antagonistic relationship, masarimycin was evaluated for its ability to interact with DNA. Masarimycin was investigated for its ability to 329 inhibit nuclease activity and intercalate DNA in established assays (Figure S7). [20, 21] 330 331 Masarimycin showed no inhibition of nuclease activity or ability to intercalate DNA, suggesting the antagonism observed is likely not due to direct interaction with DNA or nucleases. Further 332 333 the additive interaction with rifampicin (RNA synthesis) and the protein synthesis inhibitors 334 tetracycline and kanamycin in Table 2 suggests a pure summation effect of the antibiotics with masarimycin. This suggests the antagonism with levofloxacin is not a product of downstream 335 336 inhibition of transcription and translation. It should be noted that there is a connection between quinolone bactericidal activity and the expression of stress-induced proteins.[60] Cell wall 337 targeting antibiotics like β-lactams can activate the SOS response system.[61] The antagonism 338 observed with levofloxacin can be explained by the induction of the SOS system by both 339 340 compounds.[62] 341 342 343 344 345 346 347

impact PG metabolite flux through MurA/B by reducing the levels of NADPH in the cell.

Table 2. Synergy and antagonism screen with masarimycin.

Antibiotic	MIC _{app} antibiotic ^a (μΜ)	FIC antibiotic	MIC _{app} masarimycin ^ь (μΜ)	FIC masarimycin	FIC _{index}
Ampicillin	0.010	1	2	0.25	1.25
Bacitracin	1.66	0.5	15.6	2	2.5
Cefoxitin	0.69	0.4	4	0.5	0.9
Cefuroxime	0.012	1.59	2	0.25	1.75
Fosfomycin	85.87	0.5	32	4	4.5
Kanamycin	43	0.5	1.66	0.21	0.71
Levofloxacin	1.08	0.5	32	4	4.5
Optochin	7.96	0.5	8	1	1.5
Rifampicin	0.0023	0.124	3.33	0.416	0.54
Tetracycline	0.048	0.75	2	0.25	1
Vancomycin	0.003	1	4	0.5	1.5

349 350

351

352

348

353 354

355

356 357

358

359

360 361

362

363

364

365

366367

368

369

370371

Conclusion

Taking this data holistically, we posit that masarimycin activity is impacted by alterations to the cell wall caused by deletion of certain autolysins (LytB, DacA, Pmp23) in S. pneumoniae. These three autolysins are associated with remodeling PG during division (LytB)[31], or associated with division (DacA)[39] or with the Z-ring (Pmp23)[36] components of the cell division complex. Other PG hydrolases [63-65] might also be affected by masarimycin treatment, giving rise to the complex phenotypic results. The data presented here demonstrates that the morphological phenotypes of genetic knockouts of cell wall acting enzymes can be distinct from chemical inactivation and may more closely resemble the phenotype of catalytically inactive mutants. This distinction has previously been observed in *Mycobacterium tuberculosis* shikimate biosynthesis.[66] These data illustrate that the use of genetic and phenotypic screens for target identification may not always lead directly to the molecular target. The complexity involved in deciphering the underlying mechanisms associated with these meta-phenotypes obfuscates target identification. Despite these challenges, the elucidation of the molecular target of masarimycin is on-going. Based on the data provided here, masarimycin may provide a unique molecular scaffold for the development of anti-S. pneumoniae therapeutics and can play a role in furthering our understanding of PG metabolism.

 $^{^{}a}$ – MIC for antibiotics alone. ampicillin: 0.010 μM; bacitracin: 3.325 μM; cefoxitin: 1.72 μM; cefuroxime: 0.008 μM; fosfomycin: 171.5 μM; kanamycin: 86 μM; levofloxacin: 2.16 μM; optochin: 15.85 μM; rifampicin: 0.018 μM; tetracycline: 0.065 μM; vancomycin: 0.003 μM.

b-MIC masarimycin 8 μM

The bacterial cell wall and PG biosynthesis has provided a wealth of clinically relevant antibiotic targets. While our understanding of PG biosynthetic and cross-linking steps is well established, our knowledge of the role autolytic enzymes play in the growth and maintenance of the cell wall has remained more elusive. Traditional genetic approaches to studying the biological role of autolysins are complicated by functional redundancy of these enzymes, where other autolysins can compensate for a loss in activity. The results presented here illustrate the complexity of PG metabolism and the difficulty in identifying the molecular target of small molecule inhibitors. Recent reports [4, 6, 7] have begun to elucidate the role of autolysins in relieving stress in the cell wall to allow for incorporation of new material into the stress bearing layer. The results with the diamide masarimycin demonstrate that sensitivity is impacted by alterations in the cell wall caused by the deletion of specific autolysins associated with cell division and separation. Upregulation of elongation factor Tu, a moonlighting protein known to regulate cell shape, indicates that masarimycin is impacting cell wall metabolism. Collectively our data further demonstrate that morphological, genetic, and whole cell assays (autolysis) reveal metaphenotypes that result from the complex interaction of one or more cellular processes that appear connected to cell wall metabolism. The genetic deletion of one or more autolysins disrupts the equilibrium stoichiometry of the cell wall machinery that likely results in changes to expression levels and activity to both autolytic and biosynthetic enzymes. With interest in the development of chemical biology approaches to study PG metabolism[67-71] receiving renewed attention, the diamide inhibitor masarimycin provides a potential small molecule complement to both traditional genetic and current chemical biology approaches to studying cell wall metabolism.

Conflict of Interest

372

373

374

375

376377

378

379

380

381

382

383

384 385

386

387 388

389

390

391

392

393

394

395

396

397

398

399

400

401

The authors A.B. and C.W.R hold patents on specific applications of masarimycin.

Funding Information

Research was partially supported by the National Science Foundation (CHE2009522) and by the Rhode Island Institutional Development Award (IDeA) Network of Biomedical Research Excellence from the National Institute of General Medical Sciences of the National Institutes of Health under grant number P20GM103430. NMR analysis of masarimycin was supported by the National Science Foundation major research instrumentation program award under grant

- 402 number 1919644. Proteomic analysis was performed at the National Resource for Quantitative
- 403 Proteomics supported through a grant from the National Institute of General Medical Sciences
- 404 (R24GM137786).

405 Acknowledgements

406 We thank J. Belval for technical assistance.

References Cited

- 408 1. **Munita JM, Bayer AS, Arias CA**. Evolving resistance among Gram-positive pathogens.
- 409 Clin Infect Dis 2015;61(suppl_2):S48-S57.
- 410 2. Drug-resistant Streptococcus pneumoniae.
- 411 https://www.cdc.gov/drugresistance/pdf/threats-report/strep-pneumoniae-508.pdf [accessed 412 03/05/2022 2022].
- 413 3. **Koch AL, Doyle RJ**. Inside-to-outside growth and turnover of the wall of gram-positive rods. *J Theor Biol* 1985;117(1):137-157.
- 4. **Beeby M, Gumbart JC, Roux B, Jensen GJ**. Architecture and assembly of the Grampositive cell wall. *Mol Microbiol* 2013;88(4):664-672.
- 5. **Blackman SA, Smith TJ, Foster SJ**. The role of autolysins during vegetative growth of Bacillus subtilis 168. *Microbiology* 1998;144 (Pt 1):73-82.
- 419 6. Wheeler R, Turner RD, Bailey RG, Salamaga B, Mesnage S et al. Bacterial cell
- enlargement requires control of cell wall stiffness mediated by peptidoglycan hydrolases. *mBio* 2015;6(4):e00660.
- 422 7. Misra G, Rojas ER, Gopinathan A, Huang KC. Mechanical consequences of cell-wall
- turnover in the elongation of a Gram-positive bacterium. *Biophys J* 2013;104(11):2342-2352.
- 424 8. **Taguchi A, Kahne D, Walker S**. Chemical tools to characterize peptidoglycan 425 synthases. *Curr Opin Chem Biol* 2019;53:44-50.
- 426 9. **Welsh MA, Schaefer K, Taguchi A, Kahne D, Walker S**. Direction of chain growth and substrate preferences of shape, elongation, division, and sporulation-family peptidoglycan
- 428 glycosyltransferases. *J Am Chem Soc* 2019;141(33):12994-12997.
- 429 10. Rubino FA, Mollo A, Kumar S, Butler EK, Ruiz N et al. Detection of transport
- intermediates in the peptidoglycan flippase MurJ identifies residues essential for conformational cycling. *J Am Chem Soc* 2020;142(12):5482-5486.
- 432 11. Sjodt M, Brock K, Dobihal G, Rohs PDA, Green AG et al. Structure of the
- peptidoglycan polymerase RodA resolved by evolutionary coupling analysis. *Nature*
- 434 2018;556(7699):118-121.
- 435 12. Lai GC, Cho H, Bernhardt TG. The mecillinam resistome reveals a role for
- peptidoglycan endopeptidases in stimulating cell wall synthesis in Escherichia coli. *PLoS Genet* 2017;13(7):e1006934.
- 438 13. **Gautam A, Vyas R, Tewari R**. Peptidoglycan biosynthesis machinery: a rich source of drug targets. *Crit Rev Biotechnol* 2011;31(4):295-336.
- 14. Nayyab S, O'Connor M, Brewster J, Gravier J, Jamieson M et al. Diamide inhibitors
- of the Bacillus subtilis N-acetylglucosaminidase LytG that exhibit antibacterial activity. ACS
- 442 *Infect Dis* 2017;3(6):421-427.
- 443 15. Boersma MJ, Kuru E, Rittichier JT, VanNieuwenhze MS, Brun YV et al. Minimal
- 444 peptidoglycan (PG) turnover in wild-type and PG hydrolase and cell division mutants of

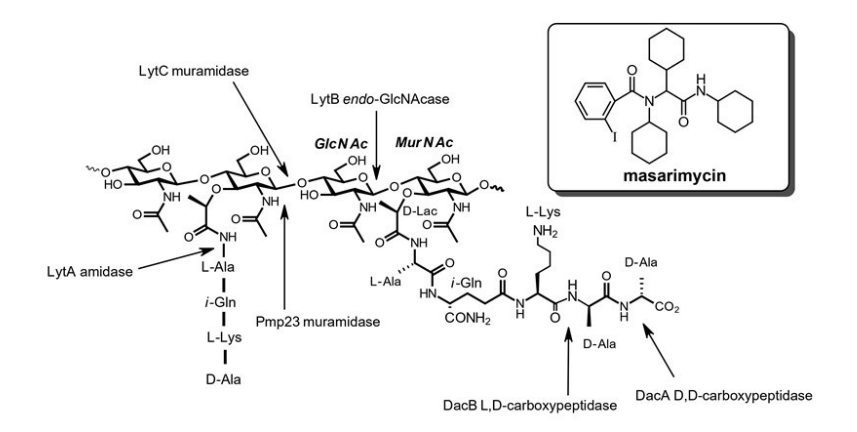
- Streptococcus pneumoniae D39 growing planktonically and in host-relevant biofilms. *J Bacteriol* 2015;197(21):3472-3485.
- 447 16. Bai X-H, Chen H-J, Jiang Y-L, Wen Z, Huang Y et al. Structure of pneumococcal
- peptidoglycan hydrolase LytB reveals insights into the bacterial cell wall remodeling and
- pathogenesis *J Biol Chem* 2014;289(34):23403-23416.
- 450 17. Palomino JC, Martin A, Camacho M, Guerra H, Swings J et al. Resazurin microtiter
- assay plate: simple and inexpensive method for detection of drug resistance in *Mycobacterium* tuberculosis. Antimicrob Agents Chemother 2002;46(8):2720-2722.
- 453 18. Czarny TL, Perri AL, French S, Brown ED. Discovery of novel cell wall-active
- compounds using PywaC, a sensitive reporter of cell wall stress, in the model Gram-positive
- bacterium Bacillus subtilis. Antimicrob Agents Chemother 2014;58(6):3261-3269.
- 456 19. **Cornett JB, Shockman GD**. Cellular lysis of *Streptococcus faecalis* induced with triton 457 X-100. *J Bacteriol* 1978;135(1):153-160.
- 458 20. Furlan RLA, Garrido LM, Brumatti G, Amarante-Mendes GP, Martins RA et al. A
- rapid and sensitive method for the screening of DNA intercalating antibiotics. *Biotechnol Lett* 2002;24(21):1807-1813.
- 461 21. Huang J, Shi J, Molle V, Sohlberg B, Weaver D et al. Cross-regulation among
- disparate antibiotic biosynthetic pathways of *Streptomyces coelicolor*. *Molecular Microbiol*
- 463 2005;58(5):1276-1287.
- 22. **Zimmerman T, Ibrahim S**. Choline kinase, a novel drug target for the inhibition of
- 465 Streptococcus pneumoniae. Antibiotics 2017;6(4).
- 466 23. Morsczeck C, Prokhorova T, Sigh J, Pfeiffer M, Bille-Nielsen M et al. Streptococcus
- 467 pneumoniae: proteomics of surface proteins for vaccine development. Clin Microbiol Infect
 468 2008;14(1):74-81.
- 24. Nesvizhskii Al, Keller A, Kolker E, Aebersold R. A statistical model for identifying
- proteins by tandem mass spectrometry. *Anal Chem* 2003;75(17):4646-4658.
- 471 25. Farha MA, Czarny TL, Myers CL, Worrall LJ, French S et al. Antagonism screen for
- inhibitors of bacterial cell wall biogenesis uncovers an inhibitor of undecaprenyl diphosphate
- 473 synthase. *Proc Nat Acad Sci U S A* 2015;112(35):11048-11053.
- 474 26. Odds FC. Synergy, antagonism, and what the chequerboard puts between them. J
- 475 Antimicrob Chemother 2003;52(1):1-1.
- 476 27. van Opijnen T, Dedrick S, Bento J. Strain dependent genetic networks for antibiotic-
- sensitivity in a bacterial pathogen with a large pan-genome. *PLoS pathogens*
- 478 2016;12(9):e1005869-e1005869.
- 479 28. Donati C, Hiller NL, Tettelin H, Muzzi A, Croucher NJ et al. Structure and dynamics of
- the pan-genome of *Streptococcus pneumoniae* and closely related species. *Genome Biol*
- 481 2010;11(10):R107.
- 482 29. Hiller NL, Janto B, Hogg JS, Boissy R, Yu S et al. Comparative genomic analyses of
- seventeen *Streptococcus pneumoniae* strains: insights into the pneumococcal supragenome. *J*
- 484 *Bacteriol* 2007;189(22):8186-8195.
- 485 30. Aaberge IS, Eng J, Lermark G, Løvik M. Virulence of Streptococcus pneumoniae in
- mice: a standardized method for preparation and frozen storage of the experimental bacterial
- 487 inoculum. *Microb Pathog* 1995;18(2):141-152.
- 488 31. Garcia P, Gonzalez MP, Garcia E, Lopez R, Garcia JL. LytB, a novel pneumococcal
- murein hydrolase essential for cell separation. *Mol Microbiol* 1999;31(4):1275-1281.
- 490 32. Rico-Lastres P, Díez-Martínez R, Iglesias-Bexiga M, Bustamante N, Aldridge C et
- **al.** Substrate recognition and catalysis by LytB, a pneumococcal peptidoglycan hydrolase
- 492 involved in virulence. *Sci Rep* 2015;5:16198-16198.
- 493 33. Lipski A, Hervé M, Lombard V, Nurizzo D, Mengin-Lecreulx D et al. Structural and
- 494 biochemical characterization of the β-N-acetylglucosaminidase from *Thermotoga maritima*:

- Toward rationalization of mechanistic knowledge in the GH73 family. *Glycobiology* 2014;25(3):319-330.
- 497 34. **Horsburgh GJ, Atrih A, Williamson MP, Foster SJ**. LytG of *Bacillus subtilis* is a novel 498 peptidoglycan hydrolase: the major active glucosaminidase. *Biochemistry* 2003;42(2):257-264.
- 499 35. **Klainer AS, Perkins RL**. Surface manifestations of antibiotic-induced alterations in protein synthesis in bacterial cells. *Antimicrob Agents Chemother* 1972;1(2):164-170.
- 36. Jacq M, Arthaud C, Manuse S, Mercy C, Bellard L et al. The cell wall hydrolase
- Pmp23 is important for assembly and stability of the division ring in *Streptococcus pneumoniae*. *Sci Rep* 2018;8(1):7591.
- 504 37. **Schuster C, Dobrinski B, Hakenbeck R**. Unusual septum formation in *Streptococcus* 505 *pneumoniae* mutants with an alteration in the D,D-carboxypeptidase penicillin-binding protein 3. 506 *J Bacteriol* 1990;172(11):6499-6505.
- 507 38. **Barendt SM, Sham L-T, Winkler ME**. Characterization of ,mutants deficient in the I,d-508 carboxypeptidase (DacB) and WalRK (VicRK) regulon, involved in peptidoglycan maturation of 509 *Streptococcus pneumoniae* serotype 2 strain D39. *J Bacteriol* 2011:193(9):2290-2300.
- 510 39. Morlot C, Noirclerc-Savoye M, Zapun A, Dideberg O, Vernet T. The d,d-
- 511 carboxypeptidase PBP3 organizes the division process of *Streptococcus pneumoniae*. *Mol Microbiol* 2004;51(6):1641-1648.
- 513 40. **Severin A, Schuster C, Hakenbeck R, Tomasz A**. Altered murein composition in a DD-
- 514 carboxypeptidase mutant of *Streptococcus pneumoniae*. *J Bacteriol* 1992;174(15):5152-5155.
- 515 41. **Höltje JV, Tomasz A**. Lipoteichoic acid: a specific inhibitor of autolysin activity in
- 516 Pneumococcus. *Proc Nat Acad Sci USA* 1975;72(5):1690-1694.
- 517 42. **Yamada S, Sugai M, Komatsuzawa H, Nakashima S, Oshida T et al.** An autolysin ring associated with cell separation of *Staphylococcus aureus*. *J Bacteriol* 1996;178(6):1565-1571.
- 519 43. Palumbo E, Deghorain M, Cocconcelli PS, Kleerebezem M, Geyer A et al. D-Alanyl
- ester depletion of teichoic acids in Lactobacillus plantarum results in a major modification of
- lipoteichoic acid composition and cell wall perforations at the septum mediated by the Acm2 autolysin. *J Bacteriol* 2006;188(10):3709-3715.
- 523 44. **Hakenbeck R, Madhour A, Denapaite D, Brückner R**. Versatility of choline metabolism
- and choline-binding proteins in *Streptococcus pneumoniae* and commensal streptococci. *FEMS Microbiol Rev* 2009;33(3):572-586.
- 526 45. **Defeu Soufo HJ**, **Reimold C**, **Linne U**, **Knust T**, **Gescher J et al.** Bacterial translation
- 527 elongation factor EF-Tu interacts and colocalizes with actin-like MreB protein. *Proc Nat Acad* 528 *Sci* 2010;107(7):3163-3168.
- 529 46. **Shelburne SA, Davenport MT, Keith DB, Musser JM**. The role of complex
- carbohydrate catabolism in the pathogenesis of invasive streptococci. *Trends Microbiol* 2008;16(7):318-325.
- 532 47. **Singh AK, Pluvinage B, Higgins MA, Dalia AB, Woodiga SA et al.** Unravelling the
- Multiple Functions of the Architecturally Intricate *Streptococcus pneumoniae* β-galactosidase, BgaA. *PLoS Pathogens* 2014;10(9):e1004364.
- 535 48. **Wang Z, Rahkola J, Redzic JS, Chi Y-C, Tran N et al.** Mechanism and inhibition of Streptococcus pneumoniae IgA1 protease. *Nat Commun* 2020;11(1):6063.
- 537 49. Jiménez-Munguía I, Pulzova L, Kanova E, Tomeckova Z, Majerova P et al.
- Proteomic and bioinformatic pipeline to screen the ligands of *S. pneumoniae* interacting with
- human brain microvascular endothelial cells. Sci Reports 2018;8(1):5231.
- 540 50. Harvey KL, Jarocki VM, Charles IG, Djordjevic SP. The Diverse Functional Roles of
- 541 Elongation Factor Tu (EF-Tu) in Microbial Pathogenesis. Front Microbiol Rev 2019;10.
- 542 51. Ling E, Feldman G, Portnoi M, Dagan R, Overweg K et al. Glycolytic enzymes
- associated with the cell surface of Streptococcus pneumoniae are antigenic in humans and elicit
- protective immune responses in the mouse. *Clin Exper Immunol* 2004;138(2):290-298.

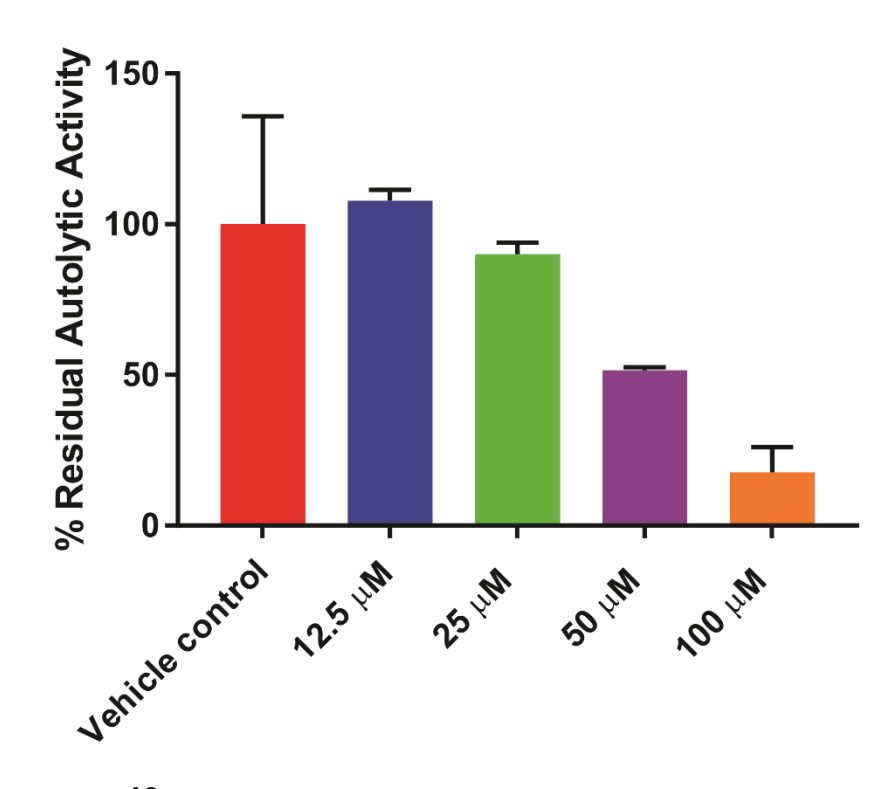
- 545 52. Wang G, Xia Y, Cui J, Gu Z, Song Y et al. The roles of moonlighting proteins in
- bacteria. Curr Issues Mol Biol 2014;16(1):15-22. 546
- 547 Mascher T, Heintz M, Zähner D, Merai M, Hakenbeck R. The CiaRH system of
- 548 Streptococcus pneumoniae prevents lysis during stress induced by treatment with cell wall
- inhibitors and by mutations in pbp2x Involved in beta-lactam resistance. J Bacteriol 549
- 550 2006;188(5):1959-1968.
- Zhou R, Chen S, Recsei P. A dye release assay for determination of lysostaphin 551 54.
- activity. Anal Biochem 1988;171(1):141-144. 552
- 553 Martin-Galiano AJ, Yuste J, Cercenado MI, de la Campa AG. Inspecting the potential
- physiological and biomedical value of 44 conserved uncharacterised proteins of Streptococcus 554
- pneumoniae. BMC Genomics 2014;15:652. 555
- Barreteau H, Kovač A, Boniface A, Sova M, Gobec S et al. Cytoplasmic steps of 556 56.
- 557 peptidoglycan biosynthesis. FEMS Microbiol Rev 2008;32(2):168-207.
- Posada AC, Kolar SL, Dusi RG, Francois P, Roberts AA et al. Importance of 558
- bacillithiol in the oxidative stress response of Staphylococcus aureus. Infect Immun 559
- 560 2014;82(1):316-332.
- Liebeke M, Meyer H, Donat S, Ohlsen K, Lalk M. A metabolomic view of 561 58.
- 562 Staphylococcus aureus and its ser/thr kinase and phosphatase deletion mutants: involvement in cell wall biosynthesis. Chem Biol 2010;17(8):820-830. 563
- 564 Courcelle J, Hanawalt PC. RecA-dependent recovery of arrested DNA replication forks.
- Annu Rev Genet 2003;37:611-646. 565
- Kohanski MA, Dwyer DJ, Collins JJ. How antibiotics kill bacteria: from targets to 566 60.
- 567 networks. Nat Rev Microbiol 2010;8(6):423-435.
- Miller C, Thomsen LE, Gaggero C, Mosseri R, Ingmer H et al. SOS response 568
- 569 induction by beta-lactams and bacterial defense against antibiotic lethality. Science
- 570 2004;305(5690):1629-1631.
- **Baharoglu Z, Mazel D**. SOS, the formidable strategy of bacteria against aggressions. 571 62.
- 572 FEMS Microbiol Rev 2014;38(6):1126-1145.
- Ng W-L, Tsui H-CT, Winkler ME. Regulation of the pspA virulence factor and essential 573
- pcsB murein biosynthetic genes by the phosphorylated VicR (YycF) response regulator in 574
- Streptococcus pneumoniae. J Bacteriol 2005;187(21):7444-7459. 575
- Dubrac S, Msadek T. Identification of genes controlled by the essential YycG/YycF two-576 64.
- 577 component system of Staphylococcus aureus. J Bacteriol 2004;186(4):1175-1181.
- Bartual SG, Straume D, Stamsås GA, Muñoz IG, Alfonso C et al. Structural basis of 578
- 579 PcsB-mediated cell separation in Streptococcus pneumoniae. Nature Commun 2014;5(1):3842.
- 580 Ramachandran V, Singh R, Yang X, Tunduguru R, Mohapatra S et al. Genetic and
- chemical knockdown: a complementary strategy for evaluating an anti-infective target. Adv Appl 581
- 582 Bioinform Chem 2013:6:1-13.
- DeMeester KE, Liang H, Zhou J, Wodzanowski KA, Prather BL et al. Metabolic 583
- incorporation of N-acetyl muramic acid probes into bacterial peptidoglycan. Curr Protoc Chem 584
- 585 Biol 2019;11(4):e74.
- Liang H, DeMeester KE, Hou CW, Parent MA, Caplan JL et al. Metabolic labelling of 586 68.
- the carbohydrate core in bacterial peptidoglycan and its applications. Nat Commun 587
- 588 2017;8:15015.
- Wang Y, Lazor KM, DeMeester KE, Liang H, Heiss TK et al. Postsynthetic 589 69.
- modification of bacterial peptidoglycan using bioorthogonal N-acetylcysteamine nalogs and 590
- 591 peptidoglycan O-acetyltransferase B. J Am Chem Soc 2017;139(39):13596-13599.
- Lebar MD, May JM, Meeske AJ, Leiman SA, Lupoli TJ et al. Reconstitution of 592
- 593 peptidoglycan cross-linking leads to improved fluorescent probes of cell wall synthesis. J Am
- Chem Soc 2014;136(31):10874-10877. 594

Dik DA, Zhang N, Chen JS, Webb B, Schultz PG. Semisynthesis of a bacterium with 595 71. non-canonical cell-wall cross-Links. J Am Chem Soc 2020;142(25):10910-10913. 596 597 Figures and Tables 598 599 Figure 1. Structure of PG showing the cleavage sites of several of the characterized autolysins 600 in *S. pneumoniae*. Inset: structure of the antimicrobial diamide masarimycin. 601 Figure 2 Screening of the diamide masarimycin against Streptococcus pneumoniae. (A) The diamide masarimycin inhibits detergent-induced autolysis in a concentration dependent manner. 602 Percent residual activity was calculated using autolysis in the absence of inhibitor set as 100%. 603 Data shown is the average of experiments performed in biological and technical triplicate. Error 604 bars denote standard deviation. (B) Activity of masarimycin against S. pneumoniae R6 autolysin 605 and cell wall biosynthesis mutants (13) to identify changes to masarimycin sensitivity. Assays 606 were run in biological triplicate and yielded the same MIC values. 607 608 Figure 3. Chain dispersing assay with S. pneumoniae TIGR4 \(\Delta \text{I/ytB} \) strain and purified recombinant LytB (rLytB, 2 μM). In the presence of 40 μM masarimycin dispersion of the ΔlytB 609 610 chain phenotype is not inhibited. Images were taken at 1000x magnification. Figure 4. Morphological analysis of S. pneumoniae △lytB mutant-[15] in the presence of sub-611 612 MIC masarimycin, the β-lactam cefoxitin (DacA/PBP3 selective) or in combination. Cells were 613 fixed in 1% formaldehyde, stained with methylene blue, and visualized using bright field 614 microscopy under oil immersion. 615 616 617 618 619 620 621 622

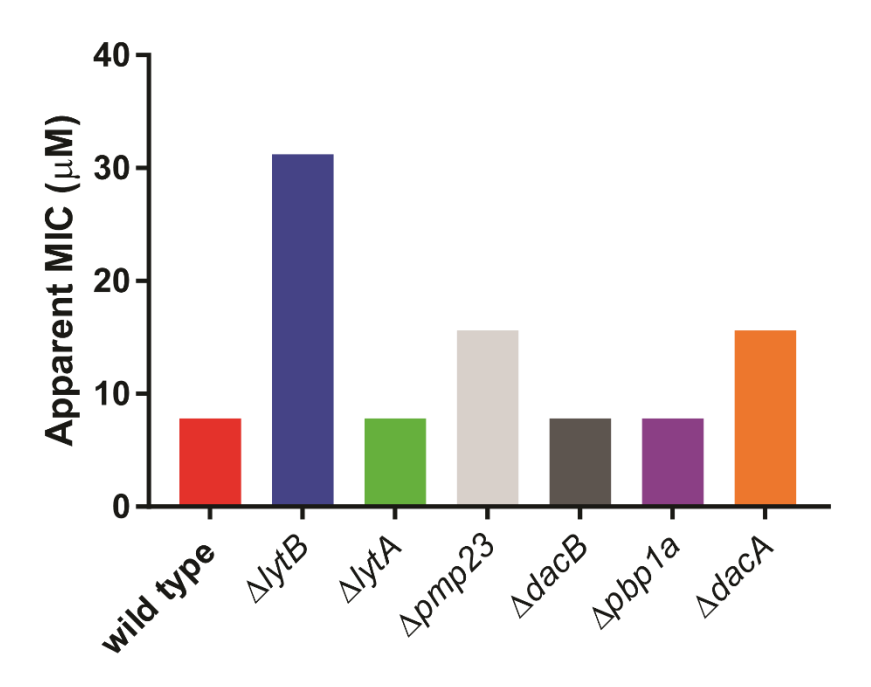
624 Figure 1.



A



В

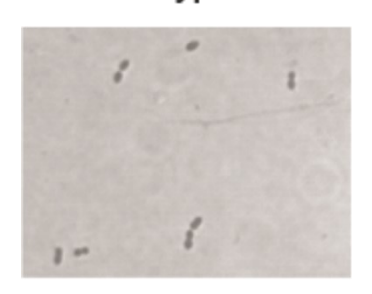


640

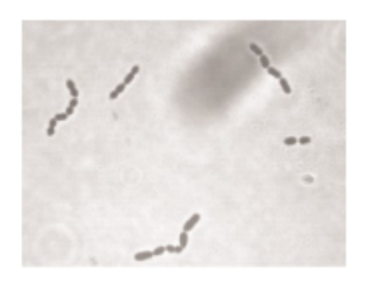
641

643 Figure 3.

wildtype



∆lytB



∆*lytB* + rLytB



∆*lytB* + rLytB + masarimycin



Figure 4.

